

Ad Hoc Adjustment of Photoredox Properties by the Late-Stage Diversification of Acridinium Photocatalysts

Valeria Hutskalova and Christof Sparr*



Cite This: *Org. Lett.* 2021, 23, 5143–5147



Read Online

ACCESS |



Metrics & More

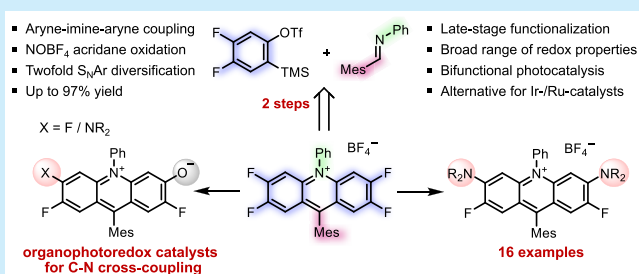


Article Recommendations



Supporting Information

ABSTRACT: The steadily growing interest in substituting precious-metal photoredox catalysts with organic surrogates is vibrantly sustained by emerging methodologies to vary their photochemical behavior. Herein, we report an ad hoc approach for the preparation of acridinium salts with a particularly broad range of photoredox properties. The method involves an aryne–imine–aryne coupling to a linchpin tetrafluoro acridinium salt for a late-stage diversification by nucleophilic aromatic substitution reactions to form diaminoacridinium and undescribed aza-rhodol photocatalysts. The different functionalities and redox properties of the organic acridinium photocatalysts render them suitable for bifunctional photoredox catalysis and organocatalytic photochemical C–N cross-couplings.



Photoredox catalysis has markedly impacted organic chemistry as a transformative strategy for molecular functionalization.^{1–3} In particular, the catalytic generation of open shell intermediates under mild reaction conditions provides a continuous impetus for conceptual advances in synthetic methodology. Due to their favorable photophysical features, ruthenium and iridium polypyridyl complexes thereby emerged as the most suitable photocatalysts (PCs).^{4,5} However, their high price and the scarcity of precious metals prompt the utilization of organic photocatalysts as a sustainable alternative.^{6–8} In recent findings, acridinium salts, introduced by Fukuzumi and refined by Nicewicz,^{9,10} stand out as a particularly advantageous class of organic photocatalysts.¹¹ To access prototypical acridinium photocatalysts, addition reactions to acridones (A)^{12–14} and Bernstein-type reactions (B) are regularly applied (Scheme 1a).¹⁵ To expand the diversity of acridinium catalysts, our group developed a route starting from esters using 1,5-bifunctional organometallic reagents (C)^{16,17} while another recent approach implements the conversion of xanthylium salts (D).¹⁸ Owing to the distinct modularity of acridinium salts, the photophysical properties can be significantly tuned by structural modifications using these catalyst preparation methodologies.¹⁹ In particular, residues directly attached to the acridinium core (R² and R³), such as amino or methoxy groups, were found to exert strong electronic effects, thereby suitably impacting the photoredox behavior of the catalysts. However, contemporary methods require the early introduction of these functionalities, necessitating multistep syntheses to alter the photoredox behavior.

We therefore envisioned that the elegant aryne–imine–aryne coupling through aza-*o*-quinone methides II formed

from 1,2-dihydrobenzoazete I as reported by Yoshida et al.²⁰ coupled with an acridane oxidation and a versatile double late-stage diversification of tetrafluoro acridinium salts by nucleophilic aromatic substitutions (S_NAr) would enable the ad hoc adjustment of the photoredox properties of acridinium catalysts 1 (Scheme 1b). While fluorine groups at the heterocyclic core were considered ideal as leaving groups for the S_NAr diversifications, it was expected that imines with a bulky mesityl group both prevent undesired 6π-electrocyclizations²⁰ and photobleaching of the anticipated catalysts.⁹

To explore the feasibility of our concept, we thus started with the preparation of the tetrafluorinated acridinium salt 4, which serves as a linchpin intermediate for the crucial late-stage diversifications (Scheme 2). Using readily available compounds 2 and 3, we embarked on optimizing the aryne–imine–aryne coupling and the ensuing acridane oxidation to form key intermediate 4 (Table S1; see the Supporting Information for details).

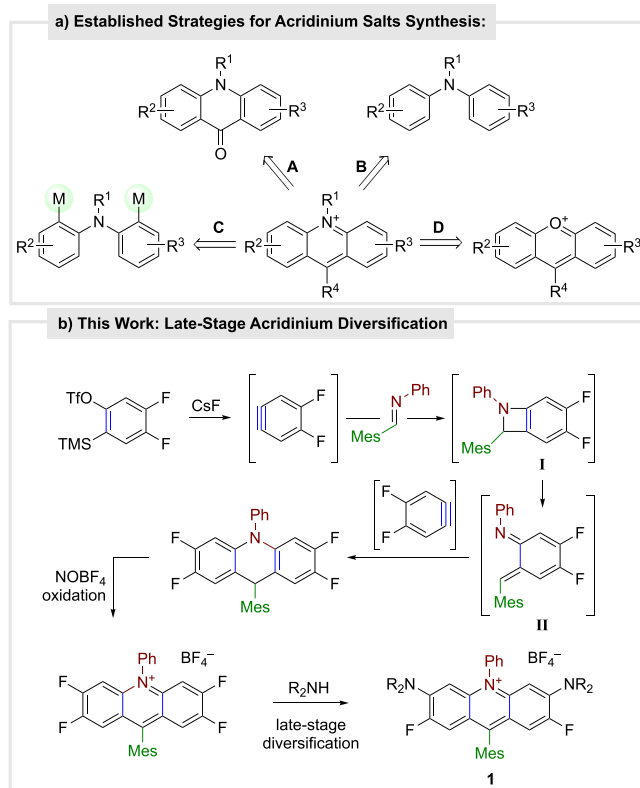
The highest yields for the aryne–imine–aryne coupling were achieved with cesium fluoride in acetonitrile, whereas nitrosonium tetrafluoroborate proved to be the most efficient reagent for the oxidation step. Interestingly, only a few examples of the application of nitrosonium salts for acridane oxidations are described in the literature,²¹ while the treatment

Received: May 18, 2021

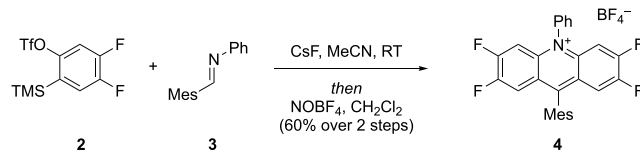
Published: June 10, 2021



Scheme 1. Background and Acridinium Diversification



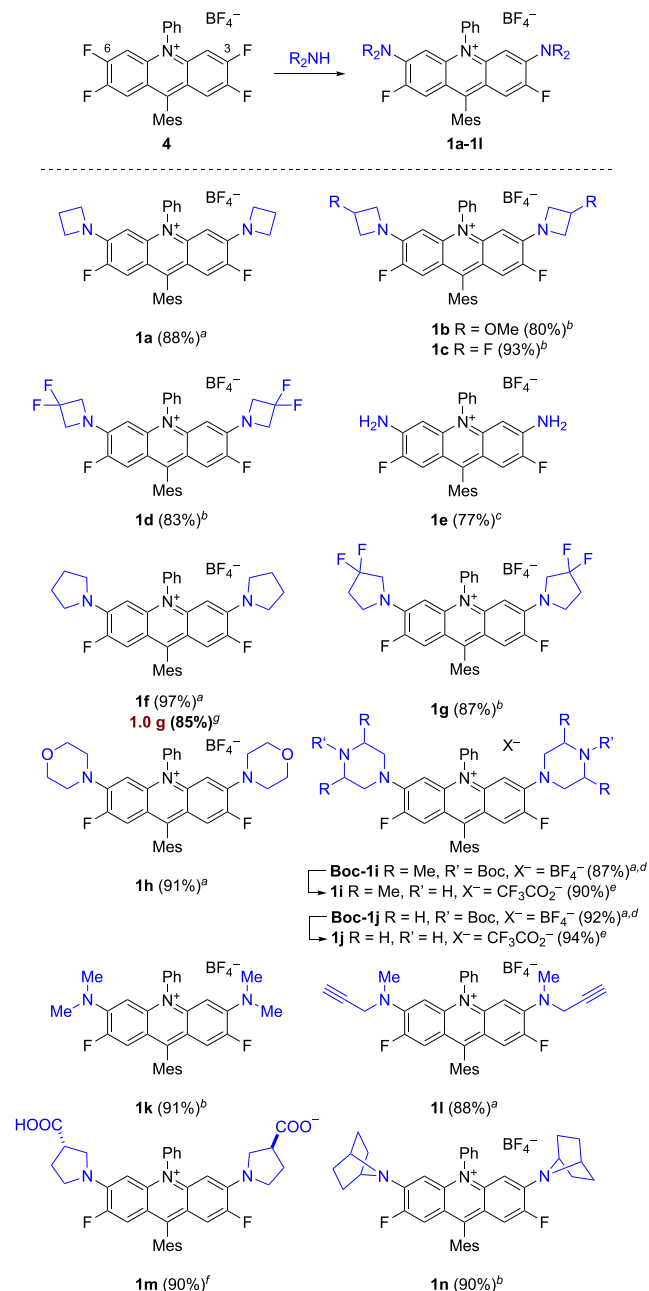
Scheme 2. Substrate Synthesis



of the acridane with chloranil, air, MnO_2 , and Bobbitt's salt resulted in either decomposition or unreacted starting material. After optimization, the two steps allowed short reaction times, an unproblematic isolation, and thus an operationally simple synthetic protocol toward the tetrafluoroacridinium salt **4** (Scheme 2).

Having acridinium intermediate **4** in hand, we focused our attention on the pivotal acridinium late-stage functionalization reactions. To test our notion of the disposition of the fluorinated acridinium core to nucleophilic attack, enabling the ad hoc preparation of photophysically distinct acridinium derivatives, we began with substitution reactions using azetidine (Scheme 3). Gratifyingly, an efficient 2-fold $\text{S}_{\text{N}}\text{Ar}$ at the most electrophilic positions (C3 and C6) was observed within 1 hour at ambient temperature, yielding desired diazetidine product **1a** in 88% yield. Interestingly, neither reduced amounts of amine nor substantial dilution led to monosubstitution. To determine the scope of this method, various amines were next subjected to the reaction. To our delight, the reactions proceeded smoothly, giving rise to the desired acridinium photocatalysts in excellent yields. Azetidines with fluorine and methoxy groups, which considerably alter the electronic properties, were readily introduced (**1a–d**). Furthermore, free amino groups were also installed by using ammonia in dioxane (**1e**). Nonetheless, all attempts to add

Scheme 3. Substrate Scope

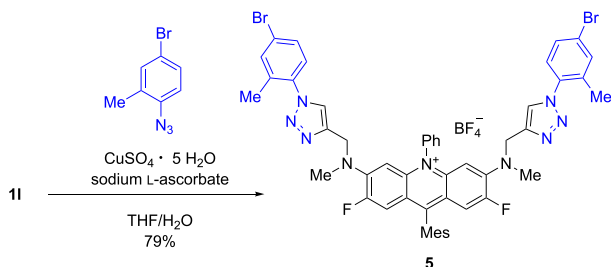


^{a–g}Yields of isolated products. Conditions: ^a**4** (47.0 μmol), R_2NH (188 μmol), CH_2Cl_2 (1.4 mL), rt; ^b**4** (47.0 μmol), $\text{R}_2\text{NH}\cdot\text{HCl}$ (470 μmol), Cs_2CO_3 (470 μmol), CH_3CN (3.3 mL), rt; ^c**4** (47.0 μmol), NH_3 (188 μmol , 0.5 M, dioxane), THF (1.5 mL); ^d**4** (90.0 μmol), R_2NH (360 μmol); ^e**Boc-1i** or **Boc-1j** (20 μmol), TFA (2.0 mL), CH_2Cl_2 (0.5 mL); ^f**4** (47.0 μmol), R_2NH (188 μmol), NEt_3 (94.0 μmol), CH_2Cl_2 (6.0 mL)/THF (2.0 mL), rt; ^g**4** (1.9 mmol).

arylamines resulted in undetectable conversions. On the contrary, selective reactions were observed for the 2-fold addition of pyrrolidines to provide **1f** or **1g** and also a gram-scale synthesis of diaminoacridinium catalyst **1f** was feasible (85% yield). The nucleophilic aromatic substitution with morpholine and Boc-piperazine led to a yield of $\geq 90\%$, and Boc deprotection reactions were readily achieved. Acyclic amines were also efficiently introduced (**1k**, 91%) even with propargylic moieties (**1l**, 88%), and the double substitutions of

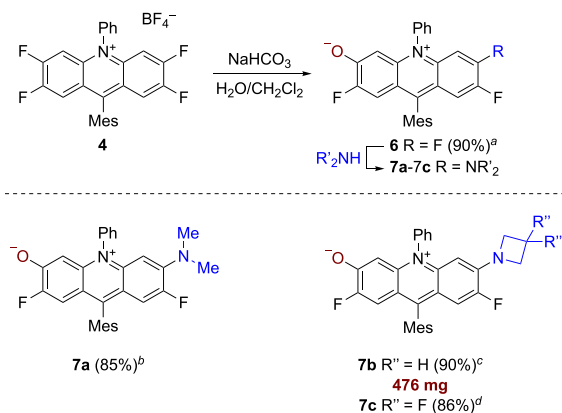
L-β-proline and 7-azabicyclo[2.2.1]heptane both proceeded with 90% isolated yield. Notably, compounds **1i** and **1m** comprise reactive functional groups that allow further manipulations, giving access to an even broader scope of applications. Indeed, acridinium salt **1i** could be effortlessly coupled by an azide–alkyne click reaction under standard conditions (Scheme 4).²² No other side products were observed after the 2-fold copper-catalyzed cycloaddition, and the desired bis-triazole acridinium compound **5** was isolated in 79% yield.

Scheme 4. Double Click Reaction with an Acridinium Salt



Captivatingly, aza-rhodols, a novel class of acridinium photoredox catalysts, could be prepared likewise by the late-stage functionalization strategy. A remarkable monohydrolysis of the linchpin tetrafluoro acridinium intermediate **4** was observed with aqueous sodium bicarbonate [**6**, 90% (Scheme 5)]. This oxygenation of the heterocycle combined with amine

Scheme 5. Synthesis of Aza-Rhodol Photoredox Catalysts



^{a–d}Yields of isolated products. ^{b–d}Yield over two steps. Reaction conditions: ^a**4** (47.0 μmol), CH_2Cl_2 (2.0 mL)/ NaHCO_3 (2.0 mL), rt, 18 h; ^b**6** (30.0 μmol), R_2NH (6.00 mmol), THF (4.0 mL), 24 h; ^c**4** (1.10 mmol), CH_2Cl_2 (50 mL)/ NaHCO_3 (100 mL), rt, 18 h, then CH_2Cl_2 (50 mL), R_2NH (15.7 mmol), 1 h, rt; ^d**6** (30.0 μmol), $\text{R}_2\text{NH}\cdot\text{HCl}$ (3.00 mmol), Cs_2CO_3 , CH_3CN (4.0 mL).

$\text{S}_{\text{N}}\text{Ar}$ reactions gave rise to aza-rhodols **7a–7c** in high overall yields. Moreover, the efficacy of this methodology was confirmed by the preparation of **7b** on a 1.1 mmol scale (90% yield).

We next examined the photophysical and electrochemical properties of acridinium salts **1a–1n**, **4**, **6**, and **7a–7c** (Table 1; see Table S4 for full details). With time-correlated single-photon counting, we were pleased to observe fluorescence lifetimes that were sufficient for photoredox catalysis for all aminoacridinium salts. Remarkably, the unique diversity of the

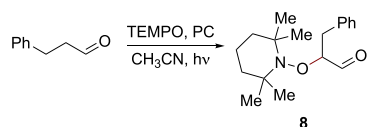
Table 1. Spectrophotometric and Electrochemical Data

PC ^a	$E_{0,0}$ (eV)	$E_{1/2}(\text{PC}/\text{PC}^-)$ (V) ^b	$E_{1/2}(\text{PC}^*/\text{PC}^-)$ (V)	τ (PC) (ns)
1a	2.40	−0.98	+1.42	3.7
1b	2.42	−0.94	+1.48	3.4
1c	2.45	−0.89	+1.56	3.4
1d	2.50	−0.80	+1.70	3.2
1e	2.63	−0.99	+1.64	3.9
1f	2.37	−0.97	+1.40	0.6 (89%)
1g	2.48	−0.85	+1.61	5.1 (54%)
1h	2.38	−0.73	+1.65	5.4 (96%)
Boc-1i	2.37	−0.73	+1.64	4.7 (56%)
Boc-1j	2.38	−0.73	+1.65	4.3 (59%)
1k	2.39	−0.89	+1.50	3.1 (89%)
1l	2.46	−0.75	+1.71	4.4 (64%)
1m	2.37	−1.06 ^c	+1.31	1.4 (48%)
1n	2.40	−0.81	+1.59	4.2
4	2.35	−0.33	+2.02	5.9 (76%)
6	2.35	−1.20	+1.15	5.4
7a	2.40	−1.36	+1.03	5.02
7b	2.42	−1.41	+1.01	4.8
7c	2.40	−1.36	+1.03	5.4 (95%)

^a $\lambda_{\text{max}}(\text{abs})$ from 458 to 513 nm; $\lambda_{\text{max}}(\text{em})$ from 494 to 551 nm; ϵ_{max} from 1.5×10^3 to $7.2 \times 10^4 \text{ L mol}^{-1} \text{ cm}^{-1}$. See the Supporting Information for the full photophysical data of the catalysts. ^bMeasured in $0.1 \text{ mol L}^{-1} n\text{-Bu}_4\text{NPF}_6$ in degassed, dry MeCN against SCE. ^cMeasured in $0.1 \text{ mol L}^{-1} n\text{-Bu}_4\text{NPF}_6$ in degassed, dry CH_3OH against SCE.

catalysts is significantly reflected by the exceptionally broad range of excited state redox potentials from an $E_{1/2}(\text{PC}^*/\text{P}^-)$ of +1.01 V (**7b**) to an $E_{1/2}(\text{PC}^*/\text{PC}^-)$ of +2.02 V (**4**). While diamino-substituted (**1a–1n**) and unsymmetric acridinium catalysts (**6** and **7a–7c**) possess redox potentials similar to those of the transition-metal-based photocatalysts [$\text{Ir}[\text{dF}(\text{CF}_3)\text{ppy}]_2(\text{dtbbpy})\text{PF}_6$ [$E_{1/2}(\text{PC}/\text{PC}^-) = -1.37 \text{ V}$; $E_{1/2}(\text{PC}^*/\text{PC}^-) = +1.21 \text{ V vs SCE}$],⁶ compound **4** shows redox potentials close to that of the Fukuzumi system [$\text{MesMeAcr}^+\text{BF}_4^-$; $E_{1/2}(\text{PC}/\text{PC}^-) = -0.57 \text{ V}$; $E_{1/2}(\text{PC}^*/\text{PC}^-) = +2.06 \text{ V vs SCE}$].¹⁵ It is thus worth pointing out that an increase in the electron-withdrawing nature of the substituents at the amine moiety generally leads to a stronger oxidative character of the excited photocatalysts, as observed for compounds **1a**, **1c**, and **1d** (Table 1). On the other hand, aza-rhodols **7a–7c** possess $E_{1/2}(\text{PC}^*/\text{PC}^-)$ and $E_{1/2}(\text{PC}/\text{PC}^-)$ values considerably lower than those of prior diaminoacridinium dyes,^{16,19} making them suitable for transformations that were unfeasible with preceding acridinium photocatalysts.

Since the diversification enabled the preparation of acridinium photocatalysts containing a variety of functional groups, including free amines (**1i** and **1j**), we explored the feasibility of an unprecedented bifunctional photocatalysis approach. Inspired by the elegant work of Akita and co-workers,²³ we thus studied the α -oxyamination of aldehydes previously utilizing a combination of amine and photoredox catalysts. To investigate bifunctional amine/acridinium catalysis (Table 2),²⁴ the activity of **1i** was compared to that of **1f** in combination with secondary amines. However, the methyl groups in **1i** and 2,6-dimethylpiperidine strongly hampered conversion. In contrast, **1f** together with morpholine as well as bifunctional aminoacridinium catalyst **1j** showed excellent catalytic activity. Under optimized conditions, full conversion

Table 2. Catalytic α -Oxyamination of Aldehydes

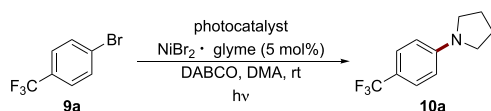
entry ^a	PC	amine	conversion ^b (%)
2	1i (8%)	–	25
3	1f (8%)	2,6-dimethylpiperidine (16%)	28
4	1f (5%)	morpholine (5%)	100
5	1j (5%)	–	83
6 ^c	1j (6%)	–	100 (84) ^d

^ahv, Kessil LED A160WE, 40 W (λ_{\max} = 464 nm). Reaction conditions: aldehyde (50.0 μ mol), TEMPO (100 μ mol), CH₃CN (0.5 mL), Ar, 18 h. ^bDetermined by NMR. ^cAt 24 h; hv, SynLED parallel photoreactor (λ = 465–470 nm). ^dIsolated yield.

and an isolated yield of 84% were conclusively obtained, confirming the aptitude of acridinium **1i** to serve as a bifunctional catalyst.

Owing to the suitably low $E_{1/2}(\text{PC}^*/\text{PC}^-)$ of aza-rhodol photocatalysts **7a–7c**, the scope for acridinium photocatalysis was distinctly expanded. These favorable properties are deemed advantageous for various catalytic applications, such as the photoredox catalytic C–N cross-coupling requiring sufficiently reducing photocatalysts [$E_{1/2}(\text{PC}^*/\text{PC}^-) \leq -1.26$ V] for precatalyst reduction [$E_i(\text{Ni}^{\text{II}}/\text{Ni}^{\text{I}}) = -1.43$ V].^{25–27} As benign alternatives to Ir and Ru catalysts,²⁸ aza-rhodols **7a–7c** with suitable redox properties were investigated (Table 3; see

Table 3. Comparison of Photoredox C–N Cross-Couplings



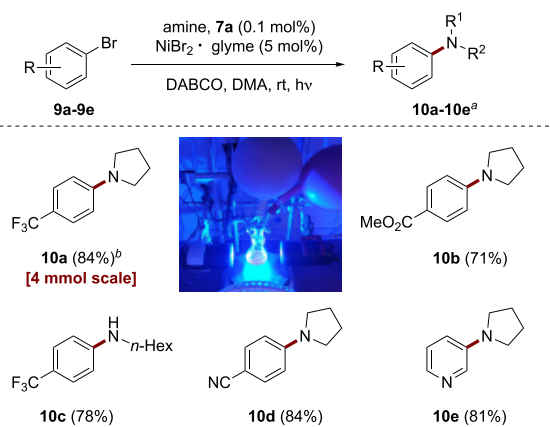
entry ^a	PC	yield ^b (%)
1	di- <i>t</i> Bu-Mes-Acr ⁺ BF ₄ [–] (0.1%)	8
2	Ir[dF(CF ₃)ppy] ₂ (dtbpy)PF ₆ (0.02%)	85
3	7a (0.02%)	75
4	7a (0.1%)	98
5	1f (0.1%)	15

^ahv, SynLED parallel photoreactor (λ = 465–470 nm). Reaction conditions: **9a** (200 μ mol), pyrrolidine (600 μ mol), NiBr₂·glyme (10.0 μ mol), DABCO (360 μ mol), DMA (1.0 mL), Ar, rt, 36 h. ^bDetermined by NMR using durenene as the standard.

Table S3 for details). In the reaction of aryl bromide **9a** with pyrrolidine, a comparison of photocatalyst (di-*t*Bu-Mes-Acr⁺BF₄[–]),³ Ir[dF(CF₃)ppy]₂(dtbpy)PF₆, aza-rhodol **7a**, and diaminoacridinium **1f** indicated the suitability of **7a** to serve as an alternative to precious metallaphotoredox catalysts.

With optimized conditions in hand, we explored the practicality and generality of aza-rhodol catalysis using different substrates (Scheme 6). We were pleased to observe that products **10a–10e** were obtained with good to excellent yields and that the robustness was confirmed by the synthesis of compound **10a** on a 4.0 mmol scale. Because oxygen and amino substituents are readily introduced during the final step, we envisage that precisely adjusted acridinium photoredox catalysts allow applications for a captivating variety of photoredox reactions.

Scheme 6. Organophotoredox C–N Cross-Coupling



Reaction conditions: aryl halide (200 μ mol), pyrrolidine (600 μ mol), NiBr₂·glyme (10.0 μ mol), DABCO (360 μ mol), **7a** (0.20 μ mol), DMA (1.0 mL), Ar, rt, 36 h; hv, SynLED Parallel Photoreactor (λ = 465–470 nm). ^aIsolated yields. ^bOn a 4 mmol scale; hv, two Kessil LED A160WE, 40 W, λ_{\max} = 464 nm.

In summary, we have developed a late-stage diversification strategy toward acridinium salts involving an aryne–imine–aryne coupling, acridane oxidation, and a versatile nucleophilic aromatic substitution reaction. The approach thereby provided 20 acridinium catalysts with a particularly broad range of redox potentials. Because of the mild reaction conditions, various functional groups were tolerated and high yields were obtained. The novel route to acridinium salts allowed the synthesis of bifunctional catalysts to efficiently merge amine and photoredox catalysis. Furthermore, the late-stage diversification approach opened access to aza-rhodol photocatalysts with uniquely low $E_{1/2}(\text{PC}^*/\text{PC}^-)$ values, enabling the replacement of precious-metal complexes in photoredox C–N cross-couplings.

■ ASSOCIATED CONTENT

Supporting Information

The Supporting Information is available free of charge at <https://pubs.acs.org/doi/10.1021/acs.orglett.1c01673>.

Experimental details and characterization data (PDF)

■ AUTHOR INFORMATION

Corresponding Author

Christof Sparr – Department of Chemistry, University of Basel, 4056 Basel, Switzerland; orcid.org/0000-0002-4213-0941; Email: christof.sparr@unibas.ch

Author

Valeriia Hutskalova – Department of Chemistry, University of Basel, 4056 Basel, Switzerland

Complete contact information is available at: <https://pubs.acs.org/doi/10.1021/acs.orglett.1c01673>

Notes

The authors declare no competing financial interest.

■ ACKNOWLEDGMENTS

The authors acknowledge the Alfred Werner Fund and the University of Basel for financial support. The authors are

grateful to Björn Pfund and Prof. Oliver S. Wenger (both University of Basel) for their advice and equipment for measuring photophysical and electrochemical data.

REFERENCES

- (1) Narayanam, J. M. R.; Stephenson, C. R. J. Visible Light Photoredox Catalysis: Applications in Organic Synthesis. *Chem. Soc. Rev.* **2011**, *40*, 102–113.
- (2) Twilton, J.; Le, C.; Zhang, P.; Shaw, M. H.; Evans, R. W.; MacMillan, D. W. C. The merger of transition metal and photocatalysis. *Nat. Rev. Chem.* **2017**, *1*, 0052.
- (3) Romero, N. A.; Nicewicz, D. A. Organic Photoredox Catalysis. *Chem. Rev.* **2016**, *116*, 10075–10166.
- (4) Yoon, T. P.; Ischay, M. A.; Du, J. Visible Light Photocatalysis as a Greener Approach to Photochemical Synthesis. *Nat. Chem.* **2010**, *2*, 527–532.
- (5) Prier, C. K.; Rankic, D. A.; MacMillan, D. W. C. Visible Light Photoredox Catalysis with Transition Metal Complexes: Applications in Organic Synthesis. *Chem. Rev.* **2013**, *113*, 5322–5363.
- (6) Fukuzumi, S.; Ohkubo, K. Organic Synthetic Transformations Using Organic Dyes as Photoredox Catalysts. *Org. Biomol. Chem.* **2014**, *12*, 6059–6071.
- (7) Hari, D. P.; König, B. Synthetic Applications of Eosin Y in Photoredox Catalysis. *Chem. Commun.* **2014**, *50*, 6688–6699.
- (8) Zilate, B.; Fischer, C.; Sparr, C. Design and Application of Aminoacridinium Organophotoredox Catalysts. *Chem. Commun.* **2020**, *56*, 1767–1775.
- (9) Fukuzumi, S.; Kotani, H.; Ohkubo, K.; Ogo, S.; Tkachenko, N. V.; Lemmetyinen, H. Electron-Transfer State of 9-Mesityl-10-Methylacridinium Ion with a Much Longer Lifetime and Higher Energy Than That of the Natural Photosynthetic Reaction Center. *J. Am. Chem. Soc.* **2004**, *126*, 1600–1601.
- (10) Kotani, H.; Ohkubo, K.; Fukuzumi, S. Photocatalytic Oxygenation of Anthracenes and Olefins with Dioxygen via Selective Radical Coupling Using 9-Mesityl-10-Methylacridinium Ion as an Effective Electron-Transfer Photocatalyst. *J. Am. Chem. Soc.* **2004**, *126*, 15999–16006.
- (11) Vega-Peñaloza, A.; Mateos, J.; Companyó, X.; Escudero-Casao, M.; Dell'Amico, L. A Rational Approach to Organo-Photocatalysis: Novel Designs and Structure-Property Relationships. *Angew. Chem., Int. Ed.* **2021**, *60*, 1082–1097.
- (12) Hamilton, D. S.; Nicewicz, D. A. Direct Catalytic Anti-Markovnikov Hydroetherification of Alkenols. *J. Am. Chem. Soc.* **2012**, *134*, 18577–18580.
- (13) Tanaka, T.; Tasaki, T.; Aoyama, Y. Acridinylresorcinol as a Self-Complementary Building Block of Robust Hydrogen-Bonded 2D Nets with Coordinative Saturation. Preservation of Crystal Structures upon Guest Alteration, Guest Removal, and Host Modification. *J. Am. Chem. Soc.* **2002**, *124*, 12453–12462.
- (14) Huang, X. Y.; Ding, R.; Mo, Z. Y.; Xu, Y. L.; Tang, H. T.; Wang, H. S.; Chen, Y. Y.; Pan, Y. M. Photocatalytic Construction of S-S and C-S Bonds Promoted by Acridinium Salt: An Unexpected Pathway to Synthesize 1,2,4-Dithiazoles. *Org. Lett.* **2018**, *20*, 4819–4823.
- (15) Joshi-Pangu, A.; Lévesque, F.; Roth, H. G.; Oliver, S. F.; Campeau, L. C.; Nicewicz, D.; DiRocco, D. A. Acridinium-Based Photocatalysts: A Sustainable Option in Photoredox Catalysis. *J. Org. Chem.* **2016**, *81*, 7244–7249.
- (16) Fischer, C.; Sparr, C. Direct Transformation of Esters into Heterocyclic Fluorophores. *Angew. Chem., Int. Ed.* **2018**, *57*, 2436–2440.
- (17) Fischer, C.; Sparr, C. Synthesis of 1,5-Bifunctional Organolithium Reagents by a Double Directed Ortho-Metalation: Direct Transformation of Esters into 1,8-Dimethoxy-Acridinium Salts. *Tetrahedron* **2018**, *74*, 5486–5493.
- (18) White, A. R.; Wang, L.; Nicewicz, D. A. Synthesis and Characterization of Acridinium Dyes for Photoredox Catalysis. *Synlett* **2019**, *30*, 827–832.
- (19) Fischer, C.; Kerzig, C.; Zilate, B.; Wenger, O. S.; Sparr, C. Modulation of Acridinium Organophotoredox Catalysts Guided by Photophysical Studies. *ACS Catal.* **2020**, *10*, 210–215.
- (20) Yoshida, H.; Kuriki, H.; Fujii, S.; Ito, Y.; Osaka, I.; Takaki, K. Aryne–Imine–Aryne Coupling Reaction via [4 + 2] Cycloaddition between Aza-*o*-Quinone Methides and Arynes. *Asian. J. Org. Chem.* **2017**, *6*, 973–976.
- (21) Suzuki, T.; Migita, A.; Higuchi, H.; Kawai, H.; Fujiwara, K.; Tsuji, T. A novel redox switch for fluorescence: drastic UV–vis and fluorescence spectral changes upon electrolysis of a hexaphenylethane derivative of 10,10'-dimethylbiacridan. *Tetrahedron Lett.* **2003**, *44*, 6837–6840.
- (22) Kumar, R.; Gahlyan, P.; Verma, A.; Jain, R.; Das, S.; Konwar, R.; Prasad, A. K. Design and Synthesis of Fluorescent Symmetric Bis-Triazolylated-1,4-Dihydropyridines as Potent Antibreast Cancer Agents. *Synth. Commun.* **2018**, *48*, 778–785.
- (23) Koike, T.; Akita, M. Photoinduced Oxyamination of Enamines and Aldehydes with TEMPO Catalyzed by [Ru(bpy)₃]²⁺. *Chem. Lett.* **2009**, *38*, 166–167.
- (24) Tagami, T.; Arakawa, Y.; Minagawa, K.; Imada, Y. Efficient Use of Photons in Photoredox/Enamine Dual Catalysis with a Peptide-Bridged Flavin-Amine Hybrid. *Org. Lett.* **2019**, *21*, 6978–6982.
- (25) Corcoran, E. B.; Pirmot, M. T.; Lin, S.; Dreher, S. D.; DiRocco, D. A.; Davies, I. W.; Buchwald, S. L.; MacMillan, D. W. C. Aryl amination using ligand-free Ni(II) salts and photoredox catalysis. *Science* **2016**, *353*, 279–283.
- (26) Till, N. A.; Tian, L.; Dong, Z.; Scholes, G. D.; MacMillan, D. W. C. Mechanistic Analysis of Metallaphotoredox C–N Coupling: Photocatalysis Initiates and Perpetuates Ni(I)/Ni(III) Coupling Activity. *J. Am. Chem. Soc.* **2020**, *142*, 15830–15841.
- (27) Wenger, O. S. Photoactive Nickel Complexes in Cross-Coupling Catalysis. *Chem. - Eur. J.* **2021**, *27*, 2270–2278.
- (28) Du, Y.; Pearson, R. M.; Lim, C. H.; Sartor, S. M.; Ryan, M. D.; Yang, H.; Damrauer, N. H.; Miyake, G. M. Strongly Reducing, Visible-Light Organic Photoredox Catalysts as Sustainable Alternatives to Precious Metals. *Chem. - Eur. J.* **2017**, *23*, 10962–10968.